

# Electronic Transport in Single-Molecule Magnets on Metallic Surfaces

Gwang-Hee Kim<sup>1\*</sup> and Tae-Suk Kim<sup>2†</sup>

<sup>1</sup>*Department of Physics, Sejong University, Seoul 143-747, Republic of Korea*

<sup>2</sup>*School of Physics, Seoul National University, Seoul 151-742, Republic of Korea*

(Received May 22, 2019)

An electron transport is studied in the system which consists of scanning tunneling microscopy-single molecule magnet-metal. Due to quantum tunneling of magnetization in single-molecule magnet, linear response conductance exhibits stepwise behavior with increasing longitudinal field and each step is maximized at a certain value of field sweeping speed. The conductance at each step oscillates as a function of the additional transverse magnetic field along the hard axis. Rigorous theory is presented that combines the exchange model with the Landau-Zener model.

PACS numbers: 75.45.+j, 75.50.Xx, 75.50.Tt

Recently high-spin molecular nanomagnets such as Mn<sub>12</sub> or Fe<sub>8</sub> attracted lots of attention due to observation of quantum tunneling of magnetization and possible applications in information storage and quantum computing[1, 2, 3, 4, 5, 6]. These single-molecule magnets (SMMs) exhibit steps in the hysteresis loops at low temperature, which is attributed to resonant tunneling between degenerate quantum states or quantum tunneling of magnetization(QTM). These unique features of SMMs are the consequence of long-living metastable spin states due to the large spin and strong anisotropy of SMMs. QTM also made it possible to detect the interference effect of Berry's phase on the magnetization at each step while the transverse field along the hard axis is varied[5, 6]. Novel features of quantum tunneling are expected to manifest themselves in, if any, other observables. Especially the effects of QTM on the electronic transport remain to be explored in both experiments[7] and theories.

In this paper we study theoretically the effects of QTM on the transport properties of SMMs which are deposited on a metallic surface with monolayer coverage. Placing the scanning tunneling microscopy(STM) tip right above one SMM, we compute the electric current which flows through a SMM when the bias voltage is applied between the STM tip and the metallic substrate(Fig. 1). We find that the linear response conductance increases stepwise like the magnetization of a SMM as a longitudinal magnetic field is increased. The stepwise behavior of conductance results from the QTM in SMM. The conductance at each step oscillates periodically as a function of additional transverse magnetic field along the hard axis. Our theoretical predictions are not known in the literature as far as we know and can be tested experimentally.

When a finite bias voltage is applied between the STM tip and the metallic substrate, the electrons will tunnel through a vacuum between the metal surface and the STM tip. Since the STM tip is placed right above the SMM in our model system, the tunneling electrons may well be scattered by the large spin of a SMM. Our model system can be considered as the conventional tunnel junction

with a SMM sandwiched between two normal metallic electrodes. The metallic substrate and STM tip are conveniently called the left( $p = L$ ) and right( $p = R$ ) electrodes, respectively. Two electrodes are described by the featureless conduction bands with the energy dispersion  $\epsilon_{pk}$ ,  $\mathcal{H}_p = \sum_{k\alpha} \epsilon_{pk} c_{pk\alpha}^\dagger c_{pk\alpha}$ . The Hamiltonian of the SMM will be introduced later. Tunneling electrons are modeled by the Hamiltonian[8, 9]

$$\mathcal{H}_1 = \sum_{kk'\alpha} \left( T_{LR} c_{Lk\alpha}^\dagger c_{Rk'\alpha} + \text{H.c.} \right) + \sum_{k\alpha} \sum_{k'\beta} \left( J_{LR} c_{Lk\alpha}^\dagger \vec{\sigma}_{\alpha\beta} c_{Rk'\beta} \cdot \vec{S} + \text{H.c.} \right), \quad (1)$$

where  $\alpha$  and  $\beta$  indicate the spin direction of electrons. The first line represents the direct tunneling between two electrodes, while the second line describes the tunneling of electrons scattered by the spin  $\vec{S}$  of SMM. Our theory is equally applicable to the molecular break junction geometry.

The electric current can be computed using the Keldysh Green's function method or equivalently the Fermi's golden rule[8]. In this paper we study the very weak coupling limit so that the higher order process like

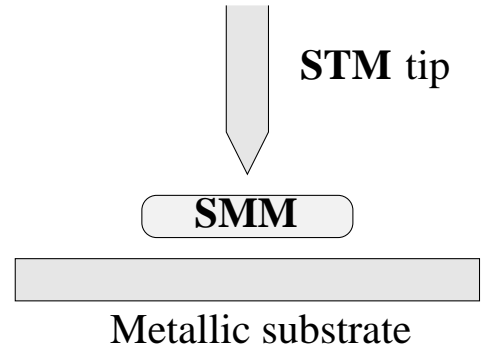


FIG. 1: Schematic diagram of our model system. A single-molecule magnet (SMM) is deposited on a metallic surface and the scanning tunneling microscopy (STM) tip is positioned right above the SMM. The easy axis of SMMs is directed normal to the metallic substrate.

the Kondo effect may be safely neglected. In this case it is enough to compute the electric current up to the leading order term. Using the Fermi's golden rule the electric current can be written as

$$I_{LR} = e \sum_m P_m \sum_{k\alpha} \sum_{k'\beta} W_{Lk\alpha m \rightarrow Rk'\beta m'} \times f(\epsilon_{Lk}) [1 - f(\epsilon_{Rk'})] - (Lk\alpha m \leftrightarrow Rk'\beta m') \quad (2)$$

Here  $W_{i \rightarrow j}$  is the transition rate from the state  $i$  to  $j$ ,  $f(\epsilon)$  is the Fermi-Dirac distribution function and  $P_m$  is the probability for the SMM to be in the state  $S_z = m$ . The leading contribution to the transition rate is given by the expression  $W_{i \rightarrow j} = \frac{2\pi}{\hbar} |\langle j | \mathcal{H}_1 | i \rangle|^2 \delta(E_i - E_j)$ , where  $i$  and  $j$  are the collective indices denoting the states  $\{Lk\alpha m\}$  or  $\{Rk'\beta m'\}$  and  $E_{p k \alpha m} = \bar{\epsilon}_{pk} + E_m$  with  $\bar{\epsilon}_{pk} = \epsilon_{pk} + \mu_p$  ( $p = L, R$ ).  $\mu_p$  is the chemical potential shift in the electrode  $p$  due to the source-drain bias voltage, and  $E_m$  is the energy of the state  $S_z = m$  in the SMM.

Up to the second order in  $T_{LR}$  and  $J_{LR}$ , we find the electric current to be

$$I_{LR} = \frac{2e^2}{h} \left[ \gamma_T + \langle S_z^2 \rangle \gamma_J \right] V + \frac{e}{h} \gamma_J \sum_m P_m [S(S+1) - m(m \pm 1)] \times [\zeta(E_m - E_{m \pm 1} + eV) - \zeta(E_m - E_{m \pm 1} - eV)]$$

where  $\gamma_T (\gamma_J) = 4\pi^2 N_L N_R |T_{LR}|^2 (|J_{LR}|^2)$  is a measure of the dimensionless direct (spin-scattered) tunneling rate,  $\langle S_z^2 \rangle = \sum_m m^2 P_m$ ,  $V$  is the source-drain bias voltage given by  $eV = \mu_L - \mu_R$ , and  $\zeta(\epsilon) = \epsilon / [1 - \exp(-\beta\epsilon)]$  with  $\beta^{-1} = k_B T$ . The linear response conductance is then  $G = \frac{2e^2}{h} \left[ \gamma_T + \gamma_J g_s(T) \right]$ , where  $g_s(T) = \langle S_z^2 \rangle + \sum_m P_m [S(S+1) - m(m \pm 1)] \eta(E_m - E_{m \pm 1})$  with  $\eta(\epsilon) = d\zeta(\epsilon)/d\epsilon$ . We would like to emphasize that only the spin-exchange tunneling reflects the dynamics of the QTM inside the SMM.

Due to the crystal electric field arising from the structure of a magnetic molecule, the ground state spin multiplet cannot remain degenerate. The effective Hamiltonian for the ground state spin multiplet of independent SMMs such as  $\text{Fe}_8$  can be expanded as[6, 11]

$$\mathcal{H}_{SMM} = -DS_z^2 + E(S_x^2 - S_y^2) + C(S_+^4 + S_-^4) - g\mu_B(H_z S_z + H_x S_x), \quad (4)$$

where  $S_x, S_y, S_z$  are three components of the spin operator,  $S_{\pm} = S_x \pm iS_y$ ,  $D$  and  $E$  are the second-order and  $C$  the fourth-order anisotropy constants, and the last term is the Zeeman energy. In the absence of transverse terms, the energy level of the state  $S_z = m$  is  $E_m = -Dm^2 - g\mu_B H_z m$ . When we start with a ground state  $S_z = -S$  corresponding to a large negative longitudinal field, the level crossing with states  $S_z = S - M$  ( $M = 0, 1, 2, \dots$ ) occurs at resonant fields,

$H_z = H_M^{(0)} = MD/g\mu_B$ . When  $H_z = H_M^{(0)}$ , the two states  $S_z = -S$  and  $S_z = S - M$  are degenerate energetically. Turning on the transverse terms leads to mixing of two degenerate states, lifts the degeneracy at the resonant fields and results in the avoided level crossing.

The scaled conductance  $g_s$  can be simplified at zero temperature by noting that  $E_S < E_{S-1} < \dots$  and  $\eta(\epsilon) = \theta(\epsilon)$ , the step function.  $g_s(M) = S^2 + \sum_{n=0}^M n P_{S-n}$ . In deriving this expression of  $g_s(M)$  it is assumed that the weight transfers from  $S_z = -S$  to  $S_z = S, S-1, \dots$  with increasing longitudinal magnetic fields.

To compute the probability, we need to solve the time-dependent Schrödinger equation for the Hamiltonian  $\mathcal{H}_{SMM}$ . The probability is defined as  $P_j \equiv \lim_{t \rightarrow \infty} |a_j(t)|^2$  when the wave function is written as  $|\Psi(t)\rangle = \sum_{j=-S}^S a_j(t) |j\rangle$ . The time-dependent Schrödinger equation for  $|\Psi(t)\rangle$  is reduced to the coupled  $2S+1$  differential equations for the coefficient  $a_j(t)$ . Recently it was numerically found[10, 11] that the two-level approximation can reproduce quite well the results of the full differential equations. In the ensuing discussion we adopt the two-level approximation to find an analytic formula of the probability. The weight transfer is found to occur only between the states  $S_z = -S$  and  $S_z = S - M$  at the resonant field  $H_M^{(0)}$ , for  $M = 0, 1, 2, \dots$ , until the complete depletion of the state  $S_z = -S$ . The amount of such weight transfer depends on the magnitude of the tunnel splitting or mixing  $\Delta_M$  between two states. At the resonant field  $H_M^{(0)}$  the full Hamiltonian  $\mathcal{H}_{SMM}$  is approximated as the effective two-level model[11, 12] between the states  $S_z = -S$  and  $S_z = S - M$ ,

$$\mathcal{H}_{\text{eff}} = \begin{pmatrix} -(S-M)g\mu_B c t & \Delta_M/2 \\ \Delta_M/2 & Sg\mu_B c t \end{pmatrix}, \quad (5)$$

where  $c (= dH_z/dt)$  is the field sweeping speed.

Defining  $\tau = g\mu_B c t / \Delta_M$  and  $\gamma_M = \hbar g\mu_B c / \Delta_M^2$ , we find the coefficient[13] around the resonant field  $H_M^{(0)}$ ,

$$a_{S-M}(\tau) = \sqrt{\lambda_M \prod_{j=0}^{M-1} F_j} \exp \left[ -\frac{1}{4} \left( i \frac{M}{\gamma_M} \tau^2 + \pi \lambda_M \right) \right] \times D_{-i\lambda_M-1} [-(1+i)\sqrt{\alpha_M} \tau], \quad (6)$$

where  $\alpha_M = (2S-M)/(2\gamma_M)$ ,  $\lambda_M = 1/(8\alpha_M \gamma_M^2)$ ,  $F_j = \exp(-2\pi\lambda_j)$  and  $D$  is the parabolic cylinder function[14]. The desired probabilities are then  $P_{S-M} = (1 - F_M) (\prod_{j=0}^{M-1} F_j)$  and  $P_{-S} = \prod_{j=0}^M F_j$ . Note that  $F_j$  and  $1 - F_j$  denote the probability for an SMM not to and to transfer from  $S_z = -S$  to  $S_z = S - j$  at the  $j$ -th resonant field, respectively. The probabilities derive from this simple observation.

To illustrate the above analytical results with concrete number, we compute the scaled conductance,  $\bar{g}_s (\equiv g_s - S^2)$  at zero temperature for an octanuclear iron(II) oxo-hydroxo cluster of formula  $[\text{Fe}_8\text{O}_2(\text{OH})_{12}(\text{tacn})_6]^{8+}$ [2].

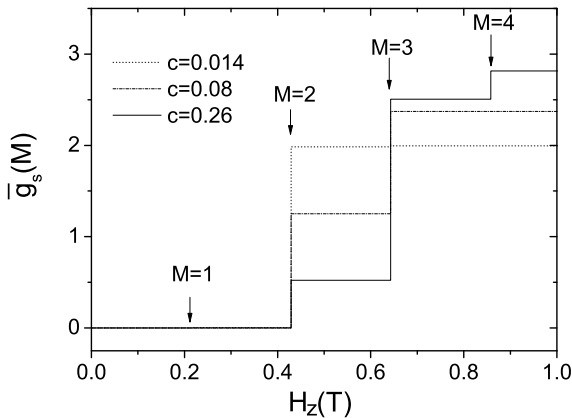


FIG. 2: The scaled conductance  $\bar{g}_s(M)$  vs. the longitudinal field  $H_z$  at zero temperature for three typical sweeping speed (T/sec).  $M = 1, 2, 3, 4$  indicate the positions of the resonant fields,  $H_M^{(0)} = 0.215, 0.429, 0.643, 0.858$ . in units of Tesla.

We adopt the model parameters from Refs. 6 and 11:  $D = 0.292\text{K}$ ,  $E = 0.046\text{K}$ ,  $C = -3.2 \times 10^{-5}\text{K}$ . The tunnel splitting  $\Delta_M$  is calculated for  $H_x = 0.1H_z$  at the resonant field by employing the numerical diagonalization[11] or the perturbation method[15]. We obtain qualitatively the same results when  $H_x$  has the fixed value at all resonant fields[16].

The scaled conductance,  $\bar{g}_s(M) = \sum_{i=1}^M \prod_{j=0}^{i-1} F_j - M \prod_{j=0}^M F_j$  which is valid for  $H_M^{(0)} \leq H_z < H_{M+1}^{(0)}$ , is displayed in Fig. 2 for three typical field sweeping speeds. Similar to the magnetization curve, the scaled conductance is featured with the stepwise increase as a function of magnetic fields. The jumps in  $\bar{g}_s(M)$  occur at the resonant fields and are caused by the QTM in SMMs. The step height is very tiny ( $\sim 0.318 \times 10^{-4}$ ) at  $H_1^{(0)} = 0.215$  T for all three sweeping speeds. At the second and third resonant fields the step heights are more pronounced and their magnitude depends sensitively on the value of  $c$ . Some steps are missing depending on both the sweeping speed and the resonant fields.

To study in more detail the structure of the steps in the conductance we plot in Fig. 3 the scaled conductance  $\bar{g}_s(M)$  at each resonant field as a function of the sweeping speed  $c$ . In comparison the magnetization,  $\langle S_z \rangle = S - \sum_{i=1}^M \prod_{j=0}^{i-1} F_j - (2S - M) \prod_{j=0}^M F_j$ , is displayed in the inset. The magnetization is a monotonically decreasing function of  $c$  while the conductance is nonmonotonic and maximized at the specific value of  $c$ . Since the weight transfer,  $1 - F_j$  at  $H_j^{(0)}$ , from  $S_z = -S$  to  $S_z = S - j$  is monotonically decreasing with increasing  $c$ , the magnetization is expected to decrease with  $c$ .

Unlike the magnetization, the conductance has contributions only from the transferred states but not from  $S_z = -S$ . Since  $F_j$  is increasing with  $c$ ,  $P_{-S}$  is an increasing function of  $c$  while  $P_{S-M}$  has the maximum

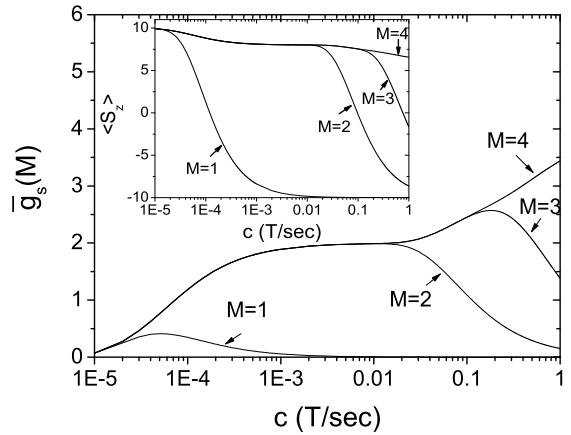


FIG. 3: Dependence of  $\bar{g}_s(M)$  on the field sweeping speed  $c$  at each resonant field. Inset: the magnetization  $\langle S_z \rangle$  vs.  $c$  at each resonant field.

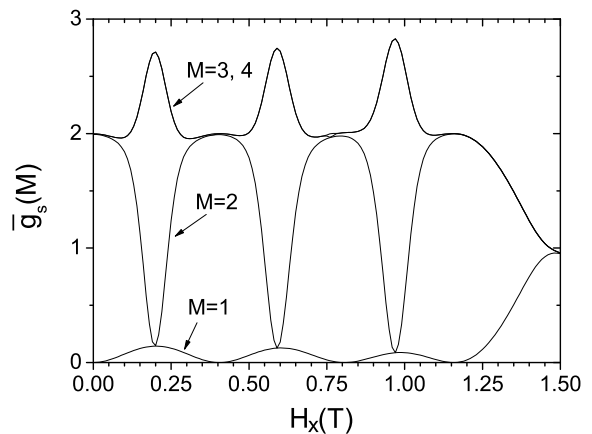


FIG. 4: Oscillation of  $\bar{g}_s(M)$  as a function of transverse field for  $c = 0.014\text{T/sec}$ . For this sweeping speed the  $M = 3, 4$  curves are almost identical except  $H_x \simeq 0, 0.4$ , and  $0.8$  T.

value as a function of  $c$ . The conductance  $\bar{g}_s(M)$  has the contribution  $\delta\bar{g}_s = MP_{S-M}$  from the  $M$ -th resonance and is expected to have the maximum value at some value of  $c$ . Such a sweeping speed can be computed approximately as  $c_M^{(\max)} \simeq [\pi/(2\hbar g\mu_B)][\Delta_M^2/(2S-M)] \log[M \sum_{i=0}^M \nu_i / (1 + \sum_{j=1}^{M-1} \sum_{i=0}^j \nu_i)]^{-1}$  where  $\nu_i = (2S)\Delta_i^2/[(2S-i)\Delta_0^2]$ . The values of  $c_M^{(\max)}$  (T/sec) are  $5.1 \times 10^{-5}$ ,  $1.08 \times 10^{-2}$ ,  $0.182$  at  $M = 1, 2, 3$ , respectively. Even though there exists a maximum in the scaled conductance at  $M = 4$ , the value of  $c = 5.16$  (T/sec) lies beyond experimentally meaningful range. In order to observe the steps in conductance at  $M = 3$  or  $M = 4$  resonance, the sweeping speed should be larger than about  $0.01$  or  $0.1$  (T/sec), respectively.

The conductances at the resonant fields are displayed in Fig. 4 as the transverse field is varied along the hard axis. Similar to the magnetization the conductance at

each resonant field oscillates with almost the same period of  $\sim 0.4$  T. Such oscillatory conductance faithfully reflects the structure of the tunnel splittings as a function of the transverse field[16]. The periodic modulation of tunnel splittings by the transverse field results from the interference between two spin paths of opposite windings around the hard axis[5, 6, 17, 18].

The tunneling splitting is known to vanish at the lattice of the diabolic fields[18]. At such fields the tunneling probability is zero so that the jump in the conductance vanishes. Depending on the parity of  $M$ , the oscillations of the conductance have the different phase. The  $M = 2$  curve is out of phase compared to the  $M = 1, 3$  curves. For example, the conductance for  $M = 2$  takes on the minimum value at the transverse field where the conductance for  $M = 1$  is maximized. This parity behavior originates from the impossibility of matching an even-valued wave function with an odd-valued one which gives rise to diabolic fields. Weak structures around  $H_x = 0$ , 0.4, and 0.8 T for  $M = 3, 4$  curves can be made conspicuous with varying the field sweeping speed. Though the overall structure of oscillatory conductance persists, the amplitude of oscillations depends sensitively on the sweeping speed[16].

We briefly address the effect of experimentally relevant issues on our theoretical results. It may be important to consider the effect of environmental degrees of freedom such as phonons, nuclear spin and dipolar interaction [19] on the magnetization process of SMMs. Such interactions make the SMM relax to the true ground state  $S_z = S$  and the relaxation process helps the magnetization to recover its full stretched value. Since all the transferred states  $S_z = S - M (M = 1, 2, \dots)$  lose the weight to the ground state, we expect that the value of  $\bar{g}_s$  will rise stepwise with increasing field and might vanish in the end due to the relaxation process. Since the elapsed time between steps, which is of the order of 10 sec or less for the typical sweeping speeds (see Fig. 2), is much smaller than the relaxation time of magnetization ( $\sim 10^4$  sec)[2, 19], we believe that the stepwise behavior of the conductance can be observed experimentally in the typical field sweeping speeds. The effect of anisotropy in SMMs on the conductance was clarified in our work. In the absence of anisotropy  $g_s = S(S + 1)$  so that the anisotropy in SMMs modifies the conductance by the amount  $S$  out of  $S(S + 1)$ . In the case of Fe<sub>8</sub> or Mn<sub>12</sub>  $S = 10$  so that the modified conductance is estimated to about 10% which lies in the experimentally detectable range. Possible exchange anisotropy in spin-scattered tunneling can be addressed[16] by considering the ratio,  $a = (J_{LR}^x + J_{LR}^y)^2 / 4[J_{LR}^z]^2$ . When  $a > 1$ , the conductance steps are more enhanced than the isotropic case ( $a = 1$ ). For the case of  $a < 1$ , the steps are reduced or can be negative depending on the value of  $a$ .

In summary we studied the current-voltage characteristics of the STM-SMM-metal system at low tempera-

ture. We found that the quantum tunneling of magnetization (QTM) in SMMs has a substantial effect on the electronic transport. The QTM in SMMs leads to the stepwise behavior in the conductance (just like the magnetization) when the magnetic field is applied along the easy axis. Unlike the magnetization the conductance at each resonance is nonmonotonic with the sweeping speed and reaches the maximum at some sweeping speed. In addition, the conductance at the resonant fields is oscillating as a function of the transverse field applied along the hard axis.

This work was supported by Korea Research Foundation Grant (KRF-2003-070-C00020), the BK21 project, and grant No. 1999-2-114-005-5 from the KOSEF.

---

\* Electronic address: gkim@sejong.ac.kr

† Electronic address: tskim@physa.snu.ac.kr

- [1] J. R. Friedman *et al.*, Phys. Rev. Lett. **76**, 3830 (1996); L. Thomas *et al.*, Nature **383**, 145 (1996).
- [2] A.-L. Barra *et al.*, Europhys. Lett. **35**, 133 (1996); C. Sangregorio *et al.*, Phys. Rev. Lett. **78**, 4645 (1997).
- [3] D. A. Garanin and E. M. Chudnovsky, Phys. Rev. B **56**, 11102 (1997); V. V. Dobrovitski and A. K. Zvezdin, Europhys. Lett. **38**, 377 (1997); L. Gunther, *ibid.*, **39**, 1 (1997); E. M. Chudnovsky and D. A. Garanin, Phys. Rev. Lett. **87**, 187203 (2001).
- [4] W. Wernsdorfer *et al.*, Nature **416**, 406 (2002); M. N. Leuenberger and D. Loss, *ibid.*, **410**, 789 (2001); J. Tejada *et al.*, Nanotechnology **12**, 181 (2001).
- [5] A. Garg, Europhys. Lett. **22**, 205 (1993).
- [6] W. Wernsdorfer and R. Sessoli, Science **284**, 133 (1999).
- [7] A. Cornia *et al.*, Angew. Chem. **42**, 1645 (2003).
- [8] J. A. Appelbaum, Phys. Rev. Lett. **17**, 91 (1966); Phys. Rev. **154**, 633 (1967).
- [9] P. W. Anderson, Phys. Rev. Lett. **17**, 95 (1966).
- [10] H. De Raedt *et al.*, Phys. Rev. B **56**, 11761 (1997).
- [11] E. Rastelli and A. Tassi, Phys. Rev. B **64**, 064410 (2001); *ibid.*, **65**, 092413 (2002).
- [12] L. Landau, Phys. Z. Sowjetunion **2**, 46 (1932); C. Zener, Proc. R. Soc. London, Ser. A, **137**, 696 (1932).
- [13] Gwang-Hee Kim (unpublished).
- [14] I. S. Gradshteyn and I. M. Ryzhik, *Table of Integrals, Series and Products* (Academic, New York, 2000).
- [15] D. A. Garanin and E. M. Chudnovsky, Phys. Rev. B **65**, 094423 (2002).
- [16] Gwang-Hee Kim and Tae-Suk Kim (unpublished).
- [17] E. M. Chudnovsky and D. P. DiVincenzo, Phys. Rev. B **48**, 10548 (1993); I. S. Tupitsyn *et al.*, Int. J. Mod. Phys. **11**, 2901 (1997); V. A. Kalatsky *et al.*, Phys. Rev. Lett. **80**, 1304 (1998).
- [18] J. Villain and A. Fort, Eur. Phys. J. B **17**, 69 (2000); A. Garg, Phys. Rev. B **64**, 094414 (2001).
- [19] A. Garg and G.-H. Kim, Phys. Rev. Lett. **63**, 2512 (1989); N. V. Prokof'ev and P. C. E. Stamp, *ibid.*, **80**, 5794 (1998); W. Wernsdorfer *et al.*, *ibid.*, **84**, 2965 (2000); L. Bokacheva *et al.*, *ibid.*, **85**, 4803 (2000); J. F. Fernández and J. J. Alonso, *ibid.*, **91**, 047202 (2003).